

Microstructure and mechanical properties of commercial purity HIPed and Crushed Aluminum

Q. H. Bui^{1,a}, G. F. Dirras^{1,b}, A. Hocini^{1,c}, S. Ramtani^{1,d}, A. Abdul-latif^{2,e}, J. Gubicza^{3,f}, T. Chauveau^{1,g}, Z. Fogarassy^{3,h}

¹LPMTM-CNRS, Université Paris 13, 99 av. JB Clément 93430 Villetaneuse, France

²L3M, IUT de Tremblay en France, Université Paris 8, rue de la Râperie, 93290 Tremblay-en-France, France

³Department of Materials Physics, Eötvös Loránd University, Budapest, P.O.B. 32, H-1518, Hungary

^abui@lpmtm.univ-paris13.fr, ^bdirras@lpmtm.univ-paris13.fr, ^chocini@lpmtm.univ-paris13.fr, ^dsalah.ramtani@lpmtm.univ-paris13.fr, ^eaabdul@iu2t.univ-paris8.fr, ^fgubicza@ludens.elte.hu, ^gchauveau@lpmtm.univ-paris13.fr, ^hfogarassyzsolt@freemail.hu

Keywords: Hot Isostatic Pressing (HIP), Dynamic severe plastic deformation (DSPD), Microstructure, ultrafine grained.

Abstract. Ultrafine-grained aluminum microstructures were processed from commercial purity powder by combining hot isostatic pressing (HIP) and dynamic severe plastic deformation (DSPD). After the first step, the bulk consolidated material showed a random texture and homogeneous microstructure of equiaxed grains with an average size of 2 μ m. The material was then subsequently impacted, using a falling weight at a strain rate of 300s⁻¹. The resulting material showed a microstructure having an average grain size of about 500 nm with a strong gradient of fiber-like crystallographic texture parallel to the impact direction. The mechanical properties of the impacted material were subsequently characterized under compressive tests at room temperature at a strain rate of 10⁻⁴s⁻¹. The effect of the change of the deformation path on the mechanical response parallel (DN) and perpendicular (DT) to the impact direction was also investigated. These results are here discussed in relation with microstructure and texture evolution.

1. Introduction

Nanocrystalline (NC) materials are one of those materials which currently receive a particular attention due to their advanced properties. These materials have been classified as microcrystalline (average grain size > 1 μ m), ultra fine-grained (UFG) with average grain size in the range 1 μ m-100nm and nanocrystalline with average grain size less than 100 nm [1].

Several procedures are now available for producing such materials including powder metallurgy (PM) [2] electro-deposition [3] and severe plastic deformation (SPD) [4-7] or a combination of different processes such as equal channel angular pressing and high pressure torsion (ECAP+HPT) [8].

The PM methods, with which one can obtain a large variety of microstructures of sub-micrometer sizes, is a versatile processing methods as, it offers a range of different compositions and grain size distributions. The UFG materials produced by such a method possess several interesting characteristics such as: isotropic crystallographic texture, low residual stress level and high fraction of high angle grain boundaries [2, 9]. However, some inherent weaknesses can be recorded such as incomplete particles bonding and porosities.

A novel experimental methodology, which aims at a grain refinement, is developed in this work. It consists to propose a two-step process where the bulk UFG aluminum is produced by a combination of PM using precisely hot isostatic pressing (HIP) and dynamic severe plastic deformation (DSPD). The new two-step process is henceforth refereed to HIP+DSPD. The resulting microstructure and its evolution during subsequent mechanical testing are studied in details.

2. Experimental procedures

The bulk material is produced by hot isostatic pressing (HIP) technique [2]. After HIP, bars of 12mm of diameter and 70 mm length are obtained. After the first step of compaction, DSPD at an average axial strain rate of 300s^{-1} is performed using the similar piece as given above. The DSPD tests are experimentally conducted using a dynamic drop mass bench of a maximum impact velocity of 10ms^{-1} and of a maximum kinetic energy of 2.5 kJ. Tests are conducted using a mass of 13.5kg.

After impact, the deformed piece has a disc shape of 22.5mm of diameter with a thickness of 6mm. This leads to a height reduction of 71%. Two samples of $3\times 3\times 5\text{ mm}^3$ were subsequently cut from the obtained disk in two different directions first, parallel (normal direction: ND) to the impact direction and secondly, perpendicular (transverse direction: TD). Then, these samples are tested under quasi-static compressive load at a strain rate of $1.6\times 10^{-4}\text{s}^{-1}$ at room temperature (RT).

To achieve the microstructure characterizations, thin foils are prepared from as-HIPed, HIP+DSPD and quasi-statically deformed HIP+DSPD samples. Initially, disks of 3mm of diameter and $70\mu\text{m}$ of thickness were cut using a Gatan™ Ultrasonic Disc Cutter and dimpled. The final thinning is carried out with a Gatan™ Precision Ion Polishing System (PIPS). Further, the microstructures were characterized by Transmission electron microscopy (TEM), using a LaB₆ JEOL™ 2011 electron microscope operating at 200 kV.

In addition to TEM investigations, X-ray Diffraction experiments (XRD) have been carried out to study the texture evolution and other parameters of interest such as crystallite sizes, dislocation density using X-ray diffraction line profile analysis. Texture measurements were performed using an Inel™ 4 circles goniometer in Bragg-Brentano geometry type with a Cobalt point focus X ray source ($\lambda=1.7902\text{ \AA}$). The measurement consisted first in the determination of the Bragg angles ($\theta/2\theta$) on the $\{111\}$, $\{200\}$, $\{220\}$ reflections and in the acquisition of the pole figures on these planes. The X-ray line profiles were measured by high-resolution rotating anode diffractometer (Nonius, FR 591). The microstructure was investigated by extended Convolutional Multiple Whole Profile (eCMWP) analysis [10,11]. In this method, the experimental pattern is fitted by the convolution of the instrumental pattern and the theoretical size and strain line profiles. Because of the ultrafine grained structure of the studied samples, the physical broadening of the profiles was much higher than the instrumental broadening; therefore, instrumental correction was not applied in the evaluation. The theoretical profile functions used in this fitting procedure are calculated on the basis of a model of the microstructure, where the crystallites have spherical shape and log-normal size distribution, and the lattice strains are assumed to be caused by dislocations.

3. Results and discussion

3.1 As-HIPed and HIP+DSPD Microstructures

A typical TEM observation of the as-HIPed microstructure is displayed in Fig. 1a. Grains are equiaxed, the interior of which is poorly populated with dislocations. The average grain size measured from TEM micrographs is about $2\mu\text{m}$ and as expected from the HIP process, the crystallographic texture is random. Fig. 1b shows the resulting microstructure after HIP+DSPD sequence observed perpendicular (TD) to the impact axis. The main characteristics of the microstructure are: (i) slightly elongated grains; (ii) average crystallites size of about 500nm that is four times lower compared to the initial average grain size of the as-HIPed material; (iii) the crystallite interiors are almost dislocation-free. These microstructures strongly suggest that a recovery and/or recrystallization processes have occurred in the course of deformation (dynamic recovery). Notice that the room temperature corresponds to $0.31T_m$ (T_m is the melting temperature) of aluminum and is within the recrystallization temperature range for pure metals ($0.3-0.4T_m$). Dynamic microstructure transformations have been frequently reported in the literature, for example in ref [12] in the case of cyclic shearing of AA-3004 alloy.

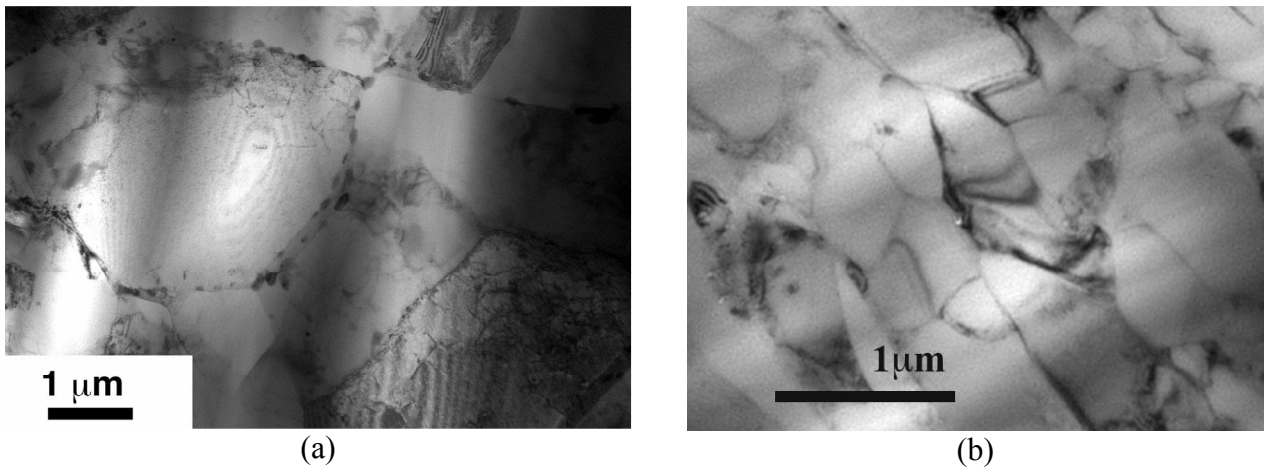


Fig. 1. (a): TEM micrograph of as-processed material by HIP ($P=200\text{MPa}$, $T=450^\circ\text{C}$, $t=240\text{min}$); (b): HIP+DSPD microstructure. (See text for details)

3.2 XRD characterizations

The three series of recalculated pole figures measured on the $\{111\}$, $\{200\}$, $\{220\}$ planes are shown in Fig. 2a and b respectively for results on the face perpendicular to the impact direction (ND) and parallel to the impact direction (TD). The analysis of the pole figures of face ND highlights the presence of a $\langle 220 \rangle$ fibre texture type noted as B. Within this fibre, a reinforcement of the intensity with a $\{011\}\langle 3\bar{2}2 \rangle$ component is found and is designated as A. The analysis of the pole figures of the TD face (Fig. 2b), still highlights the two components previously described with, however, a general decrease of the intensities. It was also found 90 degrees rotation around the longitudinal direction (DL_1) leads to a pole figure (not shown) far different to the one displayed in Fig. 2b. This highlights the presence of texture heterogeneity in the thickness of the material.

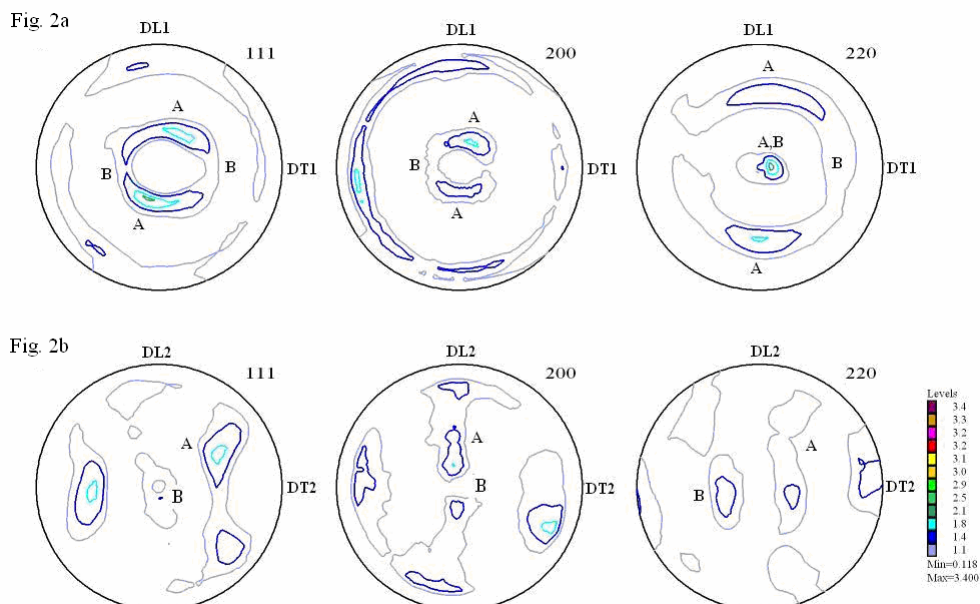


Fig. 2: Analysis of the pole figures showing the difference between ND and TD faces of the as-processed sample (see text for details).

The fitting for the HIP+DSPD sample is shown in logarithmic intensity scale in Fig. 3. The area weighted mean crystallite size and the dislocation density were determined and listed in Table 1. The measurements were carried out on both the cross-section (ND) and the transverse (TD) section. The measurements were repeated after storing the sample at RT for 1 and 3 months to check the

stability of microstructure. It seems that there is only a slight change in the microstructure during the storage of the sample at ambient conditions for three months. Notice that the dislocation density obtained is in the same order of magnitude as the saturation density ($1.8 \times 10^{14} \text{ m}^{-2}$) achieved by room temperature ECAP method [13]. The yield strength calculated from the Taylor formula using the dislocation density is 110 MPa which is in good agreement with the value determined by mechanical test (110 MPa). Moreover, this strength is also close to the value determined for the ECAP-processed sample (120 MPa). At the same time the grain size and the subgrain size (mean crystallite size) are about half of those obtained by ECAP (about 1 micron for grain size and 270 nm for crystallite size for ECAP-processed pure Al). The experimental observation that the HIP+DSPD and the ECAP sample have nearly the same dislocation densities and yield strength values, while they have different grain sizes suggests that in UFG samples processed by SPD, the yield strength is basically determined rather by the dislocation density than the grain size.

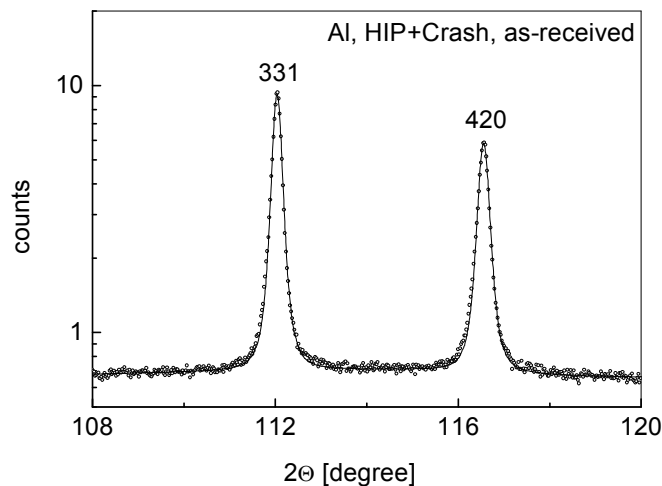


Fig. 3: A part of the experimental X-ray diffraction pattern (open circles) and the fitted curve (solid line) obtained by eCMWP fitting of X-ray line profiles method on the cross-section of the as-received sample.

Sample	mean crystallite size	dislocation density
as-received	$174 \pm 15 \text{ nm}$	$(1.4 \pm 0.2) \times 10^{14} \text{ m}^{-2}$
after 1 month at RT	$167 \pm 15 \text{ nm}$	$(1.2 \pm 0.2) \times 10^{14} \text{ m}^{-2}$
after 3 months at RT	$149 \pm 15 \text{ nm}$	$(1.0 \pm 0.2) \times 10^{14} \text{ m}^{-2}$

Table 1. The microstructure obtained by X-ray line profile analysis.

3.3 Mechanical behavior

3.3.1 Quasi-static compression testing

After DSPD, prismatic samples of square section were loaded by means of a universal testing machine under quasi-static monotonic compressive load at a strain rate of $1.6 \times 10^{-4} \text{ s}^{-1}$ at RT. Fig. 4a and 4b illustrate the mechanical behaviour after quasi-static compressive test of ND (normal direction) and TD (transverse direction) samples obtained after HIP+DSPD at 300 s^{-1} . The following observation can be made: (i) the ND sample hardens more than the TD sample, which exhibits strain localization almost just after yielding; (ii) The strength of the TD sample is lower than that of the ND sample (140 MPa for TD sample, 150 MPa for ND sample) but its yield strength is higher (120 MPa for TD sample, 110 MPa for ND sample). The different mechanical behavior is caused by the crystallographic texture in the sample.

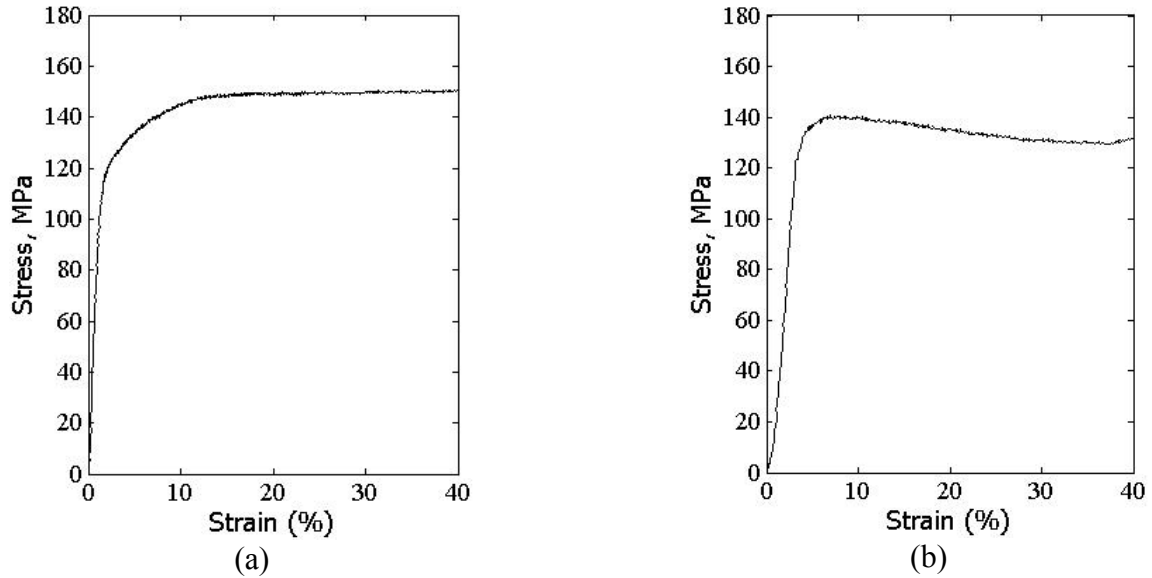


Fig. 4: True stress, true strain curves after quasi-static compressive tests of ND (a) and TD (b) samples at RT.

3.3.2 TEM investigation after compression tests at RT

Fig. 5a and 5b show TEM micrographs of sample deformed up to 40% in quasi-static compression test at RT. The grains are still equiaxed when viewed along the ND (Fig. 5a) and equiaxed but within elongated bands when viewed along TD (Fig. 5b). The majority of the grains are poorly populated with dislocations, which may explain the saturation behavior observed. At the same time it is found that the TD microstructure is very instable as it readily transforms during quasi-static compression parallel to TD. This instability is exemplified in Fig. 6 showing the occurrence of localized deformation bands, which may be the origin of the observed macroscopic softening. In addition, it has been observed that whatever orientation of the compression axis (ND or TD) the microstructure revealed several event of grains boundary bulging. At the same times, new grain orientations are locally generated, suggesting the occurrence of dynamic recrystallisation (see the center of Fig. 5a).

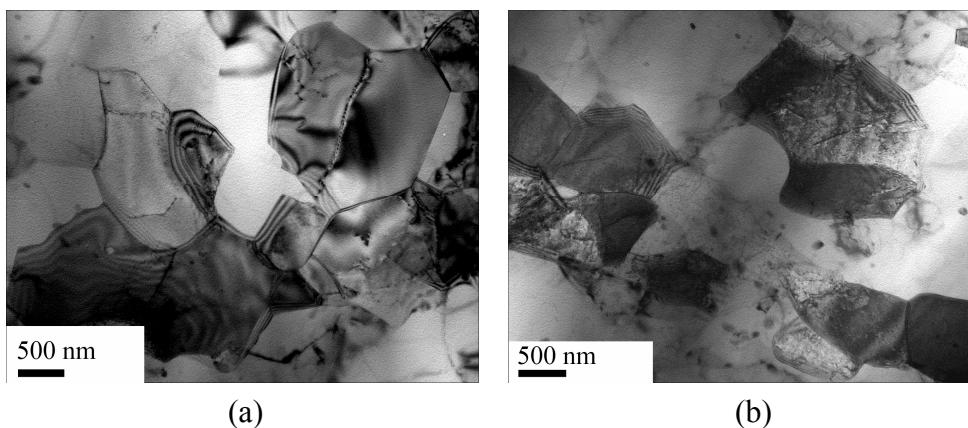


Fig 5: TEM micrographs obtained after quasi-static compression test at room temperature of ND sample (compression axis parallel to the impact direction). Thin foils are perpendicular (ND) and parallel (TD) to the compression axis respectively.

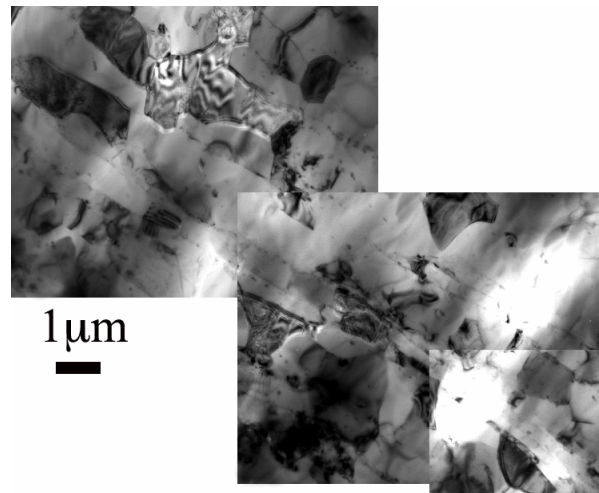


Fig 6: TEM micrographs obtained after quasi-static compression test at room temperature of TD samples. Thin foils perpendicular to the compression axis.

4. Conclusions

A new route for processing ultrafine-grained microstructures is presented. It is observed that: (i) the as-processed microstructure is comparable to that obtained by ECAP with several passes in terms of dislocation density at saturation. The crystallite size obtained after DSPS is half of that obtained by ECAP; (ii) the as-processed microstructure is stable at least at RT as revealed by XRD studies carried out after 1 and 3 months; (iii) the subsequent mechanical behaviour compares fairly well with microstructure processed by SPD; (iv) The strain path change results in softening, which can be link by an instability of the microstructure as shown by both the localization in deformation bands or enhanced dynamic recrystallisation. Nevertheless, the possible effect of the texture gradient cannot be ruled out.

References

- [1] K. S. Kumar, H. Van Swygenhoven and S. Suresh, *Acta Materialia*, 51 (2003) 5743-5774.
- [2] S. Billard, J. P. Fondère, B. Bacroix and G. F. Dirras, *Acta Materialia*, 54 (2006) 411-421.
- [3] J. Ahmad, K. Asami, A. Takeuchi, D. V. Louzguine and A. Inoue, *Mater. Trans.-Japan Inst. Met.*, 44 (2003) 1942-1947.
- [4] N. A. Smirnova, V. I. Levit, V. I. Pilyugin, R. I. Kuznetsov, L. S. Davydova and V. A. Sazonova, *Fiz. Met. Metalloved.* 61 (1986) 1170.
- [5] V. M. Segal, V. I. Reznikov, A. E. Drobyshevskiy and V. I. Kopylov, *Russ. Metall.*, 1 (1981) 99.
- [6] Y. Saito, H. Utsunomiya, N. Tsuji and T. Sakai, *Acta Mater.* 47 (1999) 579.
- [7] O. R. Valiahmetov, R. M. Galeyev and G. A. Salishchev, *Fiz. Met. Metalloved.*, 10 (1990) 204.
- [8] A. P. Zhilyaev, J. Gubicza, G. Nurislamova, Á. Révész, S. Suriñach, M. D. Baró and T. Ungár, *Phys. Stat. Sol. (a)*, 198 (2003) 263-271.
- [9] W. Q. Cao, G. F. Dirras, M. Benyoucef and B. Bacroix, *Materials Science and Engineering: A*, 462 (2007) 100-105.
- [10] G. Ribárik, J. Gubicza, T. Ungár, *Mater. Sci. Eng. A*, 387-389 (2004) 343-347.
- [11] L. Balogh, G. Ribárik, T. Ungár, *J. Appl. Phys.*, 100 (2006) 023512.
- [12] G. F. Dirras, J. L. Duval and W. Swiatnicki, *Mater. Sci. Eng. A*, 263 (1999) 85–95.
- [13] T. Ungár, J. Gubicza, *Z. Kristallographie*, 222 (2007) 114-128.